Estimation of pre-industrial nitrous oxide emissions from the land biosphere

Rongting Xu[1], Hanqin Tian[1,2], Chaoqun Lu[3], Shufen Pan[1,2], Jian Chen[4,1], Jia Yang[1], Bowen Zhang[1]

[1] International Center for Climate and Global Change Research and School of Forestry and Wildlife Sciences, Auburn University, Auburn, AL 36849, USA

[2]State Key Laboratory of Urban and Regional Ecology, Research Center for Eco-Environmental Sciences, Chinese Academy of Sciences, Beijing 100085, China

[3]Department of Ecology, Evolution, & Organismal Biology, Iowa State University, Ames, IA 50011, USA

[4] College of Sciences and Mathematics, Auburn University, Auburn, AL 36849, USA

Correspondence to: Hanqin Tian (tianhan@auburn.edu)

Abstract. To accurately assess how increased global nitrous oxide (N_2O) emission has affected the climate system requires a robust estimation of the pre-industrial N_2O emissions since only the difference between current and pre-industrial emissions represents net drivers of anthropogenic climate change. However, large uncertainty exists in previous estimates of pre-industrial N_2O emissions from the land biosphere, while pre-industrial N_2O emissions at the finer scales such as regional, biome, or sector have not yet well quantified. In this study, we applied a process-based Dynamic Land Ecosystem Model (DLEM) to estimate the magnitude and spatial patterns of pre-industrial N_2O fluxes at the biome-, continental-, and global-level as driven by multiple environmental factors. Uncertainties associated with key parameters were also evaluated. Our study indicates that the mean of the pre-industrial N_2O emission was approximately 6.20 Tg N yr^{-1}, with an uncertainty range of 4.76 to 8.13 Tg N yr^{-1}. The estimated N_2O emission varied significantly at spatial- and biome-levels. South America, Africa, and Southern Asia accounted for 34.12%, 23.85%, 18.93%, respectively, together contributing of 76.90% of global total emission. The tropics were identified as the major source of N_2O released into the atmosphere, accounting for 64.66% of the total emission. Our multi-scale estimates provide a robust reference for assessing the climate forcing of anthropogenic N_2O emission from the land biosphere

1 Introduction

Nitrous oxide (N_2O) acts as the third-most important greenhouse gas (GHG) after carbon dioxide (CO_2) and methane (CH_4), largely contributing to the current radiative forcing (Myhre et al., 2013). Nitrous oxide is also the most long-lived reactant, resulting in the destruction of stratospheric ozone (Prather et al., 2015; Ravishankara et al., 2009). The atmospheric concentration of N_2O increased from 275 to 329 parts per billion (ppb) since the pre-industrial era until 2015 at a rate of approximately 0.26% per year, as a result of human activities (Davidson, 2009; Forster et al., 2007; NOAA2006A). The human-induced N_2O emissions from the terrestrial biosphere have offset about half of terrestrial CO_2 sink and contributed a net warming effect on the climate system (Tian et al., 2016). In the contemporary period, anthropogenic N_2O emissions are mainly caused by the expansion in agricultural land area and increase in nitrogen (N) fertilizer application, as well as industrial activities, biomass burning and indirect emissions from reactive N (Galloway et al., 2004; Reay et al., 2012). Human-induced biogenic N_2O emissions were calculated by subtracting the pre-industrial emissions (Tian et al., 2016), even though a small amount of anthropogenic N_2O emissions was present before 1860, which was estimated as 1.1 Tg N yr^{-1} in 1850 by Syakila and Kroeze (2011) and 0.7 (0.6–0.8) Tg N yr^{-1} (including anthropogenic biogenic emissions from soils and biomass burning) in 1860 by Davidson (2009). Therefore, it is necessary to provide a robust reference of pre-industrial N_2O emission for assessing the climate forcing of anthropogenic N_2O emission from the land biosphere.

Numerous studies have reported the sources and estimates of N_2O emission since the pre-industrial era (Davidson and Kanter, 2014; Galloway et al., 2004; Kroeze et al., 1999; Prather et al., 2012, 2015; Syakila and Kroeze, 2011). According to the Intergovernmental Panel on Climate Change Guidelines (IPCC, 1997), the global N_2O emission evaluated by Kroeze et al. (1999) is 11 (8–13) Tg N yr^{-1} (Natural soils: 5.6–6.6 Tg N yr^{-1}, Anthropogenic: 1.4 Tg N yr^{-1}), which is consistent with the estimation from global pre-agricultural

N_2O emissions in soils (6–7 Tg N yr^{-1}) (Bouwman et al., 1993). While taking into account the new emission factor from the IPCC 2006 Guidelines (Denman et al., 2007), Syakila and Kroeze (2011) conducted an updated estimate based on the study of Kroeze et al. (1999) and reported that the global pre-industrial N_2O emission is 11.6 Tg N yr^{-1} (Anthropogenic: 1.1 Tg N yr^{-1}, Natural soils: 7 Tg N yr^{-1}). Based on the IPCC AR5, Davidson and Kanter (2014) indicated that the central estimates of both top-down and bottom-up approaches for pre-industrial natural emissions were in agreement at 11 (10–12) Tg N yr^{-1}, including natural emission from soils at 6.6 (3.3–9.0) Tg N yr^{-1} (Syakila and Kroeze, 2011). Prather et al. (2015) provided an estimate of the pre-industrial emissions (total natural emission: 10.5 Tg N yr^{-1}) based on the most recent study with a corrected lifetime of 116±9 years. Although these previous estimates intent to provide a baseline of pre-industrial N_2O emission at global-level, information on pre-industrial N_2O emissions on fine resolutions such as biome-, sector- or country-, and regional-levels remains unknown but needed for effective greenhouse gas accounting and climate policy-making.

Large uncertainties in the estimates of pre-industrial N_2O emission could derive from different approaches (i.e. top-down and bottom-up), as mentioned above. Nitrous oxide, as an important component of the N cycle, is produced by biological processes such as denitrification and nitrification in terrestrial and aquatic systems (Schmidt et al., 2004; Smith and Arah, 1990; Wrage et al., 2001). In order to accurately estimate pre-industrial N_2O emissions using the process-based Dynamic Land Ecosystem Model (DLEM, Tian et al., 2010), uncertainties associated with key parameters, such as maximum nitrification and denitrification rates, biological N fixation (BNF) rates, and the adsorption coefficient for soil ammonium (NH_4^+) and nitrate (NO_3^-), were required to be considered in model simulation. Upper and lower limits of these parameters were used to derive a range of pre-industrial N_2O emissions from terrestrial ecosystems.

In this study, the DLEM was used to simulate global N_2O emission in the pre-industrial era at a resolution of 0.5° × 0.5° latitude/longitude. Since there are no observational data of N_2O emission in the

pre-industrial period, the estimates of natural emission from Prather et al. (2012, 2015) were used to validate the simulation results. In addition, site-level N_2O emissions from different natural vegetation were used to test model performance in the contemporary period. The objectives in this study include: (1) providing a global estimation of N_2O emission from terrestrial soils in 1860, (2) offering the continental-, biome-, and country-scale N_2O emission amounts and flux rates, and (3) discussing uncertainties in estimating N_2O budget in the pre-industrial era. Finally, our estimates at global- and biome-scales were compared with previous estimates.

2 Methodology

2.1 Model description

The DLEM is a highly integrated process-based ecosystem model, which combines biophysical characteristics, plant physiological processes, biogeochemical cycles, vegetation dynamics and land use to make daily, spatially-explicit estimates of carbon, nitrogen and water fluxes and pool sizes in terrestrial ecosystems from site- and regional- to global-scales (Lu and Tian, 2013; Tian et al., 2012; Tian et al., 2015). The DLEM is characterized of cohort structure, multiple soil layer processes, coupled carbon, water and nitrogen cycles, multiple GHG emissions simulation, enhanced land surface processes, and dynamic linkages between terrestrial and riverine ecosystems (Liu et al., 2013; Tian et al., 2010, 2015). The previous results of GHG emissions from DLEM simulations have been validated against field observations and measurements at various sites (Lu and Tian, 2013; Ren et al., 2011; Tian et al., 2010, 2011; Xu et al. 2012; Zhang et al., 2016). The estimates of water, carbon, and nutrients fluxes and storages were also compared with the estimates from different approaches at regional-, continental-, and global-scales (Pan et al., 2014; Tian et al., 2015; Yang et al., 2015). Different soil organic pools and calculations of decomposition rates were described in Tian et al. (2015). The decomposition and nitrogen mineralization processes in the DLEM were described in other publications (Lu and Tian, 2013; Yang et al., 2015).

The N_2O module

Previous work provided a detailed description of trace gas modules in the DLEM (Tian et al., 2010). However, both denitrification and nitrification processes have been modified based on the first-order kinetics (Chatskikh et al., 2005; Heinen, 2006).

In the DLEM, the N_2O production and fluxes are determined by soil inorganic N content (NH_4^+ and NO_3^-) and environmental factors, such as soil texture, temperature, and moisture:

$$F_{N2O} = (R_{nit} + R_{den})F(T_{soil})(1 - F(Q_{wfp})) \quad (1)$$

where F_{N2O} is the N_2O flux from soils to the atmosphere (g N m^2 d^{-1}), R_{nit} is the daily nitrification rate (g N m^2 d^{-1}), R_{den} is the daily denitrification rate (g N m^2 d^{-1}), $F(T_{soil})$ is the function of daily soil temperature on nitrification process (unitless), and $F(Q_{wfp})$ is the function of water-filled porosity (unitless).

Nitrification, a process converting NH_4^+ into NO_3^-, is simulated as a function of soil temperature, moisture, and soil NH_4^+ concentration:

$$R_{nit} = k_{nit}F(T_{soil})F(\psi)C_{NH_4} \quad (2)$$

where k_{nit} is the daily maximum fraction of NH_4^+ that is converted into NO_3^- or gases (d^{-1}), $F(\psi)$ is the soil moisture effect (unitless), and C_{NH_4} is the soil NH_4^+ content (g N m^{-2}). Unlike Chatskikh *et al* (2005), who set k_{nit} to 0.10 d^{-1}, it varies with different plant function types (PFTs) in the DLEM with a range of 0.04 to 0.15 d^{-1}. The detailed calculations of $F(T_{soil})$ and $F(\psi)$ were described in Pan et al. (2015) and Yang et al. (2015).

Denitrification is the process that converts NO_3^- into three types of gases, namely, nitric oxide, N_2O, dinitrogen. The denitrification rate is simulated as a function of soil temperature, water-filled porosity, and NO_3^- concentration C_{NO_3} (g N g^{-1} soil):

$$R_{den} = \alpha F(T_{soil}) F(Q_{wfp}) F_N(C_{NO_3}) \quad (3)$$

where $F_N(C_{NO_3})$ is the dependency of the denitrification rate on NO_3^- concentration (unitless), and α is the maximum denitrification rate (g N m^{-2} d^{-1}). The detailed calculations of $F(Q_{wfp})$, $F_N(C_{NO_3})$ and α were described in Yang et al. (2015).

In each grid cell, there are four natural vegetation types and one crop type. The sum of N_2O emission in each grid/d^{-1} is calculated by the following formula:

$$E = \sum_{i=1}^{62481} \sum_{j=1}^{5} (N_{ij} \times f_{ij}) \times A_i \times 10^6 / 10^{12}, \ i = 1, \cdots, 62481, j = 1, \cdots, 5 \quad (4)$$

where E is the daily sum of N_2O emission from all plant functional types (PFTs) in total grids (Tg N/yr^{-1} d^{-1}); N_{ij} (g N/m^2) is the N_2O emission in the grid cell i for PFT j; f_{ij} is the fraction of cell used for PFT j in grid cell i; and A_i (km^2) is the area of the ith grid cell. 10^6 is to convert km^2 to m^2 and 10^{12} is to convert g to Tg.

2.2 Input datasets

Input data to drive DLEM simulation include static and transient data (Tian et al., 2010). Several additional data sets were generated to better represent terrestrial environment in the pre-industrial period as described below. The natural vegetation map was developed based on LUH (Hurtt et al., 2011) and SYNMAP (Jung et al., 2006), which rendered the fractions of 47 vegetation types in each 0.5° grid. These 47 vegetation types were converted to 15 PFTs used in the DLEM through a cross-walk table (Fig. 1). Cropland distribution in 1860 were developed by aggregating the 5-arc minute resolution HYDE v3.1 global cropland distribution data (Fig. 2). Half degree daily climate data (including average, maximum, minimum air temperature, precipitation, relative humidity, and shortwave radiation) were derived from CRU-NCEP climate forcing data (Wei et al., 2014). As global climate dataset was not available prior to the year 1900, long-term average climate datasets from 1901 to 1930 were used to represent the initial climate state in

1860. The nitrogen deposition dataset was developed based on the atmospheric chemistry transport model (Dentener, 2006) constrained by the EDGAR-HYDE nitrogen emission data (Aardenne et al., 2001). The nitrogen deposition dataset provided inter-annual variations of NH_x-N and NO_y-N deposition rates. The manure production dataset (1961–2013) was derived from Food and Agriculture organization of the United Nations statistic website ((FAO), http://faostat.fao.org) and defaulted for N excretion rate referred to IPCC Guidelines (Zhang et al., 2017). Estimates of manure production from 1860 to 1960 were retrieved from the global estimates in (Holland et al., 2005).

2.3 Model simulation

The implementation of the DLEM simulation includes three steps: (1) equilibrium run, (2) spin-up run, and (3) transient run. In this study, we first used land use and land cover (LULC) map in 1860, long-term mean climate during 1901–1930, N input datasets in 1860 (the concentration levels of N deposition and manure application rate), and atmospheric CO_2 in 1860 to run the model to an equilibrium state. In each grid, the equilibrium state was assumed to be reached when the inter-annual variations of carbon, nitrogen, and water storage are less than 0.1 g C/m^2, 0.1 g N/m^2 and 0.1 mm, respectively, during two consecutive 50 years. After the model reached equilibrium state, the model was spun up by the detrended climate data from 1901 to 1930 to eliminate system fluctuation caused by the model mode shift from the equilibrium to transient run (i.e., 3 spins with 10-year climate data each time). Finally, the model was run in the transient mode with daily climate data, annual CO_2 concentration, manure application, and N deposition inputs in 1860 to simulate pre-industrial N_2O emissions. Additional description of model initialization and simulation procedure can be found in previous publications (Tian et al., 2010; Tian et al., 2011).

2.4 Model validation

Observations of annual N_2O emission accumulations (g N m^{-2} yr^{-1}) were selected to compare with the simulated emissions in different sites. As there were no field measurements in the pre-industrial era, observations during 1970–2009 were collected to test the model performance in the contemporary period. All environmental factors (climate, CO_2 concentration, soil property, N deposition, LULC) in the exact year were used as input datasets for N_2O simulations. The selected 20 sites over different continents include temperate forest, tropical forest, boreal forest, savanna, and grassland. As shown in Fig. 3, the simulated N_2O emissions have a good correlation with field observations ($R^2 = 0.79$). It indicates that the DLEM has the capacity to simulate N_2O emissions in the pre-industrial era driven by environmental factors back then. The detailed information at each site can be found in Table S1.

2.5 Estimate of uncertainty

In this study, uncertainties in the simulated N_2O emission were evaluated through a global sensitivity and uncertainty analysis as described in Tian et al. (2011). Based on sensitivity analyses of key parameters that affect terrestrial N_2O fluxes, the most sensitive parameters were identified to conduct uncertainty simulations with the DLEM. These parameters include potential denitrification and nitrification rates, BNF rates, and the adsorption coefficient for soil NH_4^+ and NO_3^- (Gerber et al., 2010; Tian et al., 2015; Yang et al., 2015). The ranges of five parameters were obtained from previous studies. Chatskikh et al. (2005) set k_{nit} as 0.10 d^{-1}; however, it was set in a range of 0.04 to 0.15 d^{-1}, and varied with different PFTs in the DLEM simulations. The uncertainty ranges of potential nitrification rates were based on previous studies (Hansen, 2002; Heinen, 2006); the global pre-industrial N fixation was estimated as 58 Tg N yr^{-1}, ranging from 50–100 Tg N yr^{-1} (Vitousek et al., 2013). The spatial distribution of BNF referred to the estimates by Cleveland et al. (1999). Potential denitrification rate was set in an uncertainty range of 0.025–0.74 d^{-1}, and varied with different PFTs in the DLEM. The uncertainty ranges of the adsorption coefficient were referred to the sensitivity analysis conducted in Yang et al. (2015). Parameters used in the DLEM simulations for

uncertainty analysis were assumed to follow a normal distribution. The Improved Latin Hypercube Sampling (LHS) approach was used to randomly select an ensemble of 100 sets of parameters (R version 3.2.1) (Tian et al., 2011, 2015).

In the DLEM, after the model reached equilibrium state, a spin-up run was implemented using de-trended climate data from 1901 to 1930 for each set of parameter values. Then, each set of the model was run in transient mode in 1860 to produce the result of the pre-industrial N_2O emissions. All results from 100 groups of simulations are shown in the Table S2. The Shapiro–Wilk test was used on 100 sets of results to check the normality of DLEM simulations. It turned out that the distribution is not normal (P value < 0.05, R version 3.2.1), as shown in Fig. S1. Thus, the uncertainty range was represented as the minimum and maximum value of 100 sets of DLEM simulations.

3 Results & discussion

3.1 Magnitude and spatial distribution of the pre-industrial N_2O emission

Our estimation indicates that the global mean soil N_2O emission in the pre-industrial period (1860) was 6.20 Tg N yr^{-1}. We define the parameter-induced uncertainty of our global estimates as a range between the minimum (4.76 Tg N yr^{-1}) and the maximum (8.13 Tg N yr^{-1}) of 100 sets of DLEM simulations. The terrestrial ecosystem in the pre-industrial period acted as a source of N_2O, and its spatial pattern mostly depends on the biome distribution across the global land surface. The spatial distribution of annual N_2O emission in a 0.5° × 0.5° grid (Fig. 4) shows that the strong sources were found near the equator, such as Southeast Asia, Central Africa, and Central America, where N_2O emission reached as high as 0.45 g N m^{-2} yr^{-1}. The weak N_2O sources were observed in the northern areas of North America and Asia, where the estimated N_2O emission was less than 0.001 g N m^{-2} yr^{-1}. The microbial activity in soils determined the rate of nitrification and denitrification processes, which accounts for approximately 70% of global N_2O

emissions (Smith and Arah, 1990; Syakila and Kroeze, 2011). The tropical regions near the equator could provide microbes optimum temperatures and soil moistures to decompose soil organic matter and release more NO_x and CO_2 into the atmosphere (Butterbach-Bahl et al., 2013). Referring to the observational data from field experiments and model simulations in the tropics, it has been supported that the tropics are the main sources of N_2O emissions from natural vegetation (Bouwman et al., 1995; Werner et al., 2007; Zhuang et al., 2012).

In this study, Asia is divided into two parts: Southern Asia and Northern Asia, where the PFTs and climate conditions are significantly contrasting. As shown in Fig. 1, tropical forest and cropland were dominant PFTs in Southern Asia. In contrast, temperate and boreal forests were main PFTs in Northern Asia. The estimates of N_2O emissions from seven land regions are shown in Fig. 5. At continental scale, the N_2O emission was 2.09 (1.63–2.73) Tg N yr^{-1} in South America, 1.46 (1.13–1.91) Tg N yr^{-1} in Africa, and 1.16 (0.90–1.52) Tg N yr^{-1} in Southern Asia. South America, Africa, and Southern Asia accounted for 33.77%, 23.60%, 18.73%, respectively, together which was 76.10% of global total emission. Europe and Northern Asia contributed to 0.45 (0.32–0.66) Tg N yr^{-1}, which was less than 10% of the total emission.

Nitrous oxide emissions varied remarkably among different ecosystems. Forest, grassland, shrub, tundra and cropland contributed 76.90%, 3.11%, 13.14%, 0.18% and 6.67%, respectively, to the total emission globally (Fig. 6). In different biomes, the tropics accounted for more than half of the total N_2O emission, which is comparable to the conclusion made by Bouwman et al. (1993). In the pre-industrial era, the major inputs of reactive N to terrestrial ecosystems were from BNF, which relies on the activity of a phylogenetically diverse list of bacteria, archaea and symbioses (Cleveland et al., 1999; Vitousek et al., 2013). Tropical savannas have been considered as ‘hot spots’ of BNF by legume nodules that provide the major input of available N (Bate and Gunton, 1982). The substantial inputs of N into tropical forests could contribute to higher amount of the gaseous N losses as N_2O or nitrogen gas (Cleveland et al., 2010; Hall

and Matson, 1999). In contrast, as the largest terrestrial biome, boreal forests lack of available N because the rate of BNF is constricted by cold temperatures and low precipitation during growing season (Alexander and Billington, 1986). Morse et al. (2015) conducted field experiments in Northeastern North American forests. They found that denitrification does vary coherently with patterns of N availability in forests, and no significant correlations between atmospheric N deposition, potential net N mineralization and nitrification rates. Thus, it is reasonable that boreal forests contributed to the least amount of N_2O emission among different forests.

As shown in Fig. 2, cropland areas varied spatially. The regions with high cropland area include the entire Europe, India, eastern China, and central-eastern United States. The global N_2O emission from croplands was estimated as 0.41 (0.32–0.55) Tg N yr^{-1}, which is about ten times less than the estimate reported in the IPCC AR5 (Ciais et al., 2014). As no synthetic N fertilizer was applied to the cropland in 1860, leguminous crops were the major source of N_2O emission from croplands, most of which were planted in central-eastern United States (Fig. 4). Rochette et al. (2004) conducted the experiments on the N_2O emission from soybean without application of N fertilizer. Their work was in agreement with the suggestion that legumes may increase N_2O emissions compared with non-BNF crops (Duxbury et al., 1982) The background emission from ground-based experiments was as high as 0.31–0.42 kg N ha^{-1} in Canada (Duxbury et al., 1982; Rochette et al., 2004).

Pre-industrial N_2O emission at country-level could serve as a reference for calculating human-induced N_2O emission in today's nations. We estimated pre-industrial N_2O emissions from seventeen countries that are "hot spots" of N_2O sources in the contemporary period (Table 1). The order of countries was referred to Gerber et al. (2016) that indicated the top seventeen countries in terms of total N application in 2000. Pre-industrial N_2O emissions from natural soils and croplands varied significantly at country-scales. The United States, China, and India were top countries accounted for emissions from pre-industrial croplands.

Countries close to or located in the tropics, such as Mexico, Indonesia, and Brazil, accounted for negligible emissions from croplands, but substantial amount from natural vegetation in the pre-industrial era. Previous studies indicated that agriculture produces the majority of anthropogenic N_2O emissions (Ciais et al., 2014; Davidson and Kanter, 2014). Our estimate at country-scales could be used as a reference to quantify the net increase of N_2O emissions from agriculture activities in countries of "hot spots".

There is a debate that the natural wetlands and peatlands act as sinks or sources of N_2O. Previous studies showed that N_2O emissions from natural peatlands are usually negligible; however, the drained peatlands with lower water tables might act as sources of N_2O (Augustin et al., 1998; Martikainen et al., 1993). High water tables in wetlands might block the activity of nitrifiers and limit the denitrification (Bouwman et al., 1993). The fluxes of N_2O were negligible in the pelagic regions of boreal ponds and lakes due to the limitation of nitrification and/or nitrate inputs (Huttunen et al., 2003). Couwenberg et al. (2011) mentioned that N_2O emissions always decreased after rewetting when conducting field experiments, which had been excluded from their future analysis of GHG emissions in peatlands. Hadi et al. (2005) pointed out that tropical peatlands ranged from sources to sinks of N_2O, highly affected by land-use and hydrological zone. We were incapable to examine N_2O fluxes from wetlands and peatlands in 1860 as human-induced land-use in those ecosystems was unknown. Thus, we excluded the N_2O emissions from wetlands and peatlands in this study.

3.2 Revisit preindustrial global N_2O emission by incorporating top-down estimates

"Top-down" methodology used to estimate N_2O emissions is based on atmospheric measurements and an inversion model (Thompson et al. 2014). Prather et al. (2012) provided an estimate of 9.1±1.0 Tg N yr^{-1} of natural emission in the pre-industrial era using observed pre-industrial abundances of 270 ppb and model estimates of lifetime decreased from 142 years in the pre-industrial era to 131±10 years in the present-day. Later, Prather et al. (2015) re-evaluated N_2O lifetime based on Microwave Limb Sounder satellite

measurements of stratospheric, which was consistent with modeled values in the present-day. The lifetime in the pre-industrial era and present-day was estimated to be 123 and 116±9 years, respectively. The current lifetime increases the pre-industrial natural emission from 9.1±1.0 to 10.5 Tg N yr^{-1}.

Natural sources for N_2O include soil under natural vegetation, oceans, and atmospheric chemistry (Ciais et al., 2014). The emission from atmospheric chemistry was estimated as 0.6 with an uncertainty range of 0.3–1.2 Tg N yr^{-1}. Syakila and Kroeze (2011) estimated global natural emissions from oceans as 3.5 Tg N yr^{-1}. Oceanic emission was estimated as 3.8 with an uncertainty range of 1.8–5.8 Tg N yr^{-1} in the IPCC AR4. However, the uncertainty range became larger (1.8–9.4 Tg N yr^{-1}) in the IPCC AR5. In our study, the simulated N_2O emission was from agricultural and natural soils. The natural emission was estimated as 5.78 (4.4–7.72) Tg N yr^{-1}. Combining the atmospheric chemistry and the ocean emissions in the IPCC AR5 with the natural emissions from our study, the global total natural N_2O emissions were 10.18 (6.5-18.32) Tg N yr^{-1}. The large uncertainty range was attributed to the uncertainty from oceanic emission, atmospheric chemistry emission, and our estimation. The estimated global total amount (10.18 Tg N yr^{-1}) in this study was comparable to the estimate (10.5 Tg N yr^{-1}) by Prather et al. (2015) using the top-down approach.

3.3 Comparison with estimates by bottom-up methodology

"Bottom-up" approach includes the estimations based on inventory, statistical extrapolation of local flux measurements, and process-based modeling (Tian et al., 2016). The global pre-agricultural N_2O emission was estimated as 6.8 Tg N yr^{-1} based on the regression relationship between measured N_2O fluxes and modeled N_2O production indices (Bouwman et al., 1993). This estimate was adopted to retrieve the trends of atmospheric N_2O concentration in Syakila and Kroeze (2011). In our study, the pre-industrial N_2O emission from natural vegetation was estimated as 5.78 (4.4–7.72) Tg N yr^{-1}, which is about 1 Tg N yr^{-1}

lower than the estimate from Bouwman et al. (1993). Estimate from the tropics (± 30° of the equator) was about 4.57 Tg N yr^{-1}, which is 0.83 Tg N yr^{-1} lower than the estimate from Bouwman et al. (1993). For the rest of natural vegetation, our estimate was 1.21 Tg N yr^{-1}, which is close to 1.4 Tg N yr^{-1} estimated in Bouwman et al. (1993).

Although Bouwman et al. (1993) has studied the potential N_2O emission from natural soils, our study provided a first estimate of spatially distributed N_2O emission in 1860 using the biogeochemical process-based model. Bouwman et al. (1993) provided 1° × 1° monthly N_2O emission using the monthly controlling factors without considering the impact of N deposition. In their study, the soil fertility and carbon content were constant for every month, which could not reflect the monthly dynamic changes of carbon and N pools in natural soils. Moreover, although their study has represented a spatial distribution of potential N_2O emission from natural soils, they had not provided the estimate at biome-, continent-, and country-scales. Thus, their result was hardly to be used as a regional reference for the net human-induced N_2O emissions from some "hot spots", such as Southern Asia. In contrast, in our study, using daily climate and N deposition dataset could better reflect the real variation of N_2O emission through the growing season in natural ecosystems. The comparison with field observations during 1997–2001 indicated that the DLEM can catch the daily peak N_2O emissions in Hubbard Brook Forest (Tian et al., 2010) and Inner-Mongolia (Tian et al., 2011).

As far as the N_2O emission from croplands, our estimate is comparable to the estimate of 0.3 (0.29–0.35) Tg N yr^{-1} extracted from Syakila and Kroeze (2011) by digitizing graphs using the Getdata Graph Digitizer. In their study, the estimation was based on the relationship between the crop production and human population during 1500–1970. In contrast, the result in our study was estimated based on the cropland area of specific crop type, mainly soybean, rice, corn, and wheat in 1860.

317 Thus, the DLEM is capable to provide the estimate of N_2O emission from natural ecosystems at
318 regional- and biome-scales with a higher spatial resolution. This could be a useful reference for quantifying
319 effects of human activities such as the LULC change, N fertilizer and manure application, and increasingly
320 atmospheric N deposition on N_2O emissions in different terrestrial ecosystems or sectors in the
321 contemporary period.

322 **3.4 The N_2O budget in the pre-industrial era**

323 The observed N_2O concentration reflects the result of dynamic production and consumption processes in
324 soils as soils act as sources or sinks of N_2O through denitrification and nitrification (Chapuis-Lardy et al.,
325 2007). There was a slight increase of atmospheric N_2O concentration during 1750–1860 according to the
326 ice core records, but showed a rapid increase from 1860 to present (Ciais et al., 2014). Nature sources of
327 N_2O emissions have been discussed in section 3.2 & 3.3. Previous studies found that there were some
328 anthropogenic N_2O emissions along with the natural sources in the pre-industrial era (Davidson, 2009;
329 Syakila and Kroeze, 2011). Syakila and Kroeze (2011) found anthropogenic N_2O emission began since
330 1500 because of the biomass burning and agriculture. The total anthropogenic N_2O emission in their study
331 was estimated as 1.1 Tg N in 1850. In addition, Davidson (2009) derived a time-course analysis of sources
332 and sinks of atmospheric N_2O since 1860. The pre-industrial anthropogenic N_2O sources in his study
333 included biomass burning, agriculture (e.g. manure application, and the cultivation of legume) and human
334 sewage, the sum of which was 0.7 (0.6–0.8) Tg N yr^{-1} (Davidson, 2009). Thus, anthropogenic N_2O
335 emission has already existed in 1860, but in a small magnitude as compared with the contemporary amount.

336 Davidson (2009) mentioned that there was possibly a certain amount of N_2O loss in the pre-industrial
337 period through atmospheric sink and the reduced emission from tropical deforestation. He estimated the
338 anthropogenic sink as 0.26 Tg N in 1860. In addition, the deforestation of tropical forest might have caused
339 a loss of N_2O emissions in 1860, which was estimated as 0.03 Tg N (Davidson, 2009). However, studies

have shown that the conversion of forest to pasture and cropland could increase or have no effect on N_2O emissions because the effects depended on disturbance intensity of human activities on soil conditions (van Lent et al., 2015). For instance, N_2O emissions tended to increase during the first 5–10 years after conversion and thereafter might decrease to average upland forest or low canopy forest levels in the non-fertilized croplands and pastures. In contrast, emissions were at a high level during and after fertilization in fertilized croplands (van Lent et al., 2015). Thus, more work is needed to study how forest degradation affects N_2O fluxes (Mertz et al., 2012).

3.5 Future research needs

Large uncertainty still exists in the DLEM simulation associated with the quality of input datasets and parameters applied in simulations. Although input datasets could play a significant role in the variety of the model output, it is difficult to obtain accurate datasets back to the year 1860. Average climate data from 1901 to 1930 was used to run model simulation, which could raise the uncertainty in estimating N_2O emission in 1860. The datasets of LULC, N deposition, and manure application in 1860 could introduce uncertainties to this estimate. The average oceanic and atmospheric chemistry emissions cited from the IPCC AR5 could introduce the uncertainty into calculation of the total natural emissions in 1860 when comparing with the estimate done by Prather et al. (2015). Thus, more accurate estimate of oceanic N_2O emission is significant to narrow the confidence estimate of the pre-industrial terrestrial sources. The N_2O fluxes from wetlands and peats needed to be included in the future study.

4 Conclusions

Using the process-based land ecosystem model DLEM, this study provides a spatially-explicit estimate of pre-industrial N_2O emissions for major PFTs and critical regions across global land surface. Improved LHS was performed to analyze uncertainty ranges of the estimates. We estimated that pre-industrial N_2O

emission is 6.20 Tg N yr^{-1}. The modeled results showed a large spatial variability due to variations in climate conditions and PFTs. Tropical ecosystem was the dominant contributor of global N_2O emissions. In contrast, boreal regions contributed less than 5% to the total emission. China, India and United States are top countries accounted for emissions from croplands in 1860. While uncertainties still exist in the N_2O emission estimation in the pre-industrial era, this study offered a relatively reasonable estimate of the pre-industrial N_2O emission from land soils. Meanwhile, this study provided a spatial estimate for N_2O emission from the global hot spots, which could be used as a reference to estimate net human-induced emissions in the contemporary period.

Author Contributions

Tian H., Pan, S., and Xu, R. initiated this research and designed model simulations. Xu R. performed DLEM simulations, analyses and calculations. Lu C. contributed to the model calibration and data analysis. Chen J. contributed to the data processing and statistical analysis. Yang J. took charge of input datasets preparation (environmental factors), data description, and model verification. Zhang B. provided manure N input data. All coauthors contribute manuscript development.

Acknowledgements

This work was supported by National Science Foundation (NSF) Grants (1243232, 121036), Chinese Academy of Sciences STS Program (KFJ-STS-ZDTP-010-05) and Auburn University IGP Program. We wish to thank the previous members in the Ecosystem Dynamics and Global Ecology (EDGE) Laboratory who made great contributions to the improvements and developments of the DLEM and associated geo-referenced data set in the past decade.

References

Aardenne, J. V., Dentener, F., Olivier, J., Goldewijk, C., and Lelieveld, J.: A 1× 1 resolution data set of historical anthropogenic trace gas emissions for the period 1890–1990, Global Biogeochemical Cycles, 15, 909-928, 2001.

Alexander, V., and Billington, M.: Nitrogen fixation in the Alaskan taiga, in: Forest ecosystems in the Alaskan taiga, Springer, 112-120, 1986.

Augustin, J., Merbach, W., Steffens, L., and Snelinski, B.: Nitrous oxide fluxes of disturbed minerotrophic peatlands, Agribiological Research, 51, 47-57, 1998.

Bate, G., and Gunton, C.: Nitrogen in the Burkea savanna, in: Ecology of tropical savannas, Springer, 498-513, 1982.

Bouwman, A., Fung, I., Matthews, E., and John, J.: Global analysis of the potential for N_2O production in natural soils, Global Biogeochemical Cycles, 7, 557-597, 1993.

Bouwman, A., Van der Hoek, K., and Olivier, J.: Uncertainties in the global source distribution of nitrous oxide, Journal of Geophysical Research: Atmospheres, 100, 2785-2800, 1995.

Breuer, L., Papen, H., and Butterbach- Bahl, K.: N_2O emission from tropical forest soils of Australia, Journal of Geophysical Research: Atmospheres, 105, 26353-26367, 2000.

Butterbach-Bahl, K., Gasche, R., Huber, C., Kreutzer, K., and Papen, H.: Impact of N-input by wet deposition on N-trace gas fluxes and CH_4-oxidation in spruce forest ecosystems of the temperate zone in Europe, Atmospheric Environment, 32, 559-564, 1998.

Butterbach-Bahl, K., Baggs, E. M., Dannenmann, M., Kiese, R., and Zechmeister-Boltenstern, S.: Nitrous oxide emissions from soils: how well do we understand the processes and their controls?, Phil. Trans. R. Soc. B, 368, 20130122, 2013.

Chapuis- Lardy, L., Wrage, N., Metay, A., CHOTTE, J. L., and Bernoux, M.: Soils, a sink for N2O? A review, Global Change Biology, 13, 1-17, 2007.

Chatskikh, D., Olesen, J. E., Berntsen, J., Regina, K., and Yamulki, S.: Simulation of effects of soils, climate and management on N_2O emission from grasslands, Biogeochemistry, 76, 395-419, 2005.

Chen, G. X., Huang, B., Xu, H., Zhang, Y., Huang, G., Yu, K., Hou, A., Du, R., Han, S., and VanCleemput, O.: Nitrous oxide emissions from terrestrial ecosystems in China, Chemosphere-Global Change Science, 2, 373-378, 2000.

Ciais, P., Sabine, C., Bala, G., Bopp, L., Brovkin, V., Canadell, J., Chhabra, A., DeFries, R., Galloway, J., Heimann, M. and Jones, C.: Carbon and other biogeochemical cycles. In Climate Change 2013: The Physical Science Basis. Contribution of Working Group I to the Fifth Assessment Report of the Intergovernmental Panel on Climate Change. Cambridge University Press, 465-570, 2014.

Cleveland, C. C., Townsend, A. R., Schimel, D. S., Fisher, H., Howarth, R. W., Hedin, L. O., Perakis, S. S., Latty, E. F., Von Fischer, J. C., and Elseroad, A.: Global patterns of terrestrial biological nitrogen (N_2) fixation in natural ecosystems, Global Biogeochemical Cycles, 13, 623-645, 1999.

Cleveland, C. C., Houlton, B. Z., Neill, C., Reed, S. C., Townsend, A. R., and Wang, Y.: Using indirect methods to constrain symbiotic nitrogen fixation rates: a case study from an Amazonian rain forest, Biogeochemistry, 99, 1-13, 2010.

Couwenberg, J., Thiele, A., Tanneberger, F., Augustin, J., Bärisch, S., Dubovik, D., Liashchynskaya, N., Michaelis, D., Minke, M., and Skuratovich, A.: Assessing greenhouse gas emissions from peatlands using vegetation as a proxy, Hydrobiologia, 674, 67-89, 2011.

Davidson, E. A., Ishida, F. Y., and Nepstad, D. C.: Effects of an experimental drought on soil emissions of carbon dioxide, methane, nitrous oxide, and nitric oxide in a moist tropical forest, Global Change Biology, 10, 718-730, 2004.

Davidson, E. A.: The contribution of manure and fertilizer nitrogen to atmospheric nitrous oxide since 1860, Nature Geoscience, 2, 659-662, 2009.

Davidson, E. A., and Kanter, D.: Inventories and scenarios of nitrous oxide emissions, Environmental Research Letters, 9, 105012, 2014.

Dentener, F.: Global maps of atmospheric nitrogen deposition, 1860, 1993, and 2050, Data set. Available on-line (http://daac. ornl. gov/) from Oak Ridge National Laboratory Distributed Active Archive Center, Oak Ridge, TN, USA, 2006.

Denman K., Brasseur G., Chidthaisong A., Ciais P. M., Cox P., Dickinson R., Hauglustaine D., Heinze C., Holland E., Jacob D., Lohmann U., Ramachandran S., da Silva Dias P., Wofsy S. and Zhang X.: Couplings Between Changes in the Climate System and Biogeochemistry. In: Climate Change 2007: The Physical Science Basis. Contribution of Working Group I to the Fourth Assessment Report of the Intergovernmental Panel on Climate Change [Solomon S., Qin D., Manning M., Chen Z., Marquis M., Averyt K. B., Tignor M., and Miller H. (eds.)]. Cambridge University Press, Cambridge, United Kingdom and New York, NY, USA, 501-566, 2007.

Duxbury, J., Bouldin, D., Terry, R., and Tate, R. L.: Emissions of nitrous oxide from soils, 1982.

Eickenscheidt, N., and Brumme, R.: NO_x and N_2O fluxes in a nitrogen-enriched European spruce forest soil under experimental long-term reduction of nitrogen depositions, Atmospheric Environment, 60, 51-58, 2012.

Erickson, H., Keller, M., and Davidson, E. A.: Nitrogen oxide fluxes and nitrogen cycling during postagricultural succession and forest fertilization in the humid tropics, Ecosystems, 4, 67-84, 2001.

Erickson, H. E., and Perakis, S. S.: Soil fluxes of methane, nitrous oxide, and nitric oxide from aggrading forests in coastal Oregon, Soil Biology and Biochemistry, 76, 268-277, 2014.

Forster, P., Ramaswamy, V., Artaxo, P., Berntsen, T., Betts, R., Fahey, D. W., Haywood, J., Lean, J., Lowe, D. C., and Myhre, G.: Changes in atmospheric constituents and in radiative forcing. Chapter 2, in: Climate Change 2007. The Physical Science Basis, 2007.

Galloway, J. N., Dentener, F. J., Capone, D. G., Boyer, E. W., Howarth, R. W., Seitzinger, S. P., Asner, G. P., Cleveland, C., Green, P., and Holland, E.: Nitrogen cycles: past, present, and future, Biogeochemistry, 70, 153-226, 2004.

Gerber, S., Hedin, L. O., Oppenheimer, M., Pacala, S. W., and Shevliakova, E.: Nitrogen cycling and feedbacks in a global dynamic land model, Global Biogeochemical Cycles, 24, 2010.

Gerber, J. S., Carlson, K. M., Makowski, D., Mueller, N. D., Garcia de Cortazar- Atauri, I., Havlík, P., Herrero, M., Launay, M., O'Connell, C. S., and Smith, P.: Spatially explicit estimates of N_2O emissions from croplands suggest climate mitigation opportunities from improved fertilizer management, Global Change Biology, 2016.

Goodroad, L., and Keeney, D.: Nitrous oxide emission from forest, marsh, and prairie ecosystems, Journal of Environmental Quality, 13, 448-452, 1984.

Hadi, A., Inubushi, K., Purnomo, E., Razie, F., Yamakawa, K., and Tsuruta, H.: Effect of land-use changes on nitrous oxide (N_2O) emission from tropical peatlands, Chemosphere-Global Change Science, 2, 347-358, 2000.

Hadi, A., Inubushi, K., Furukawa, Y., Purnomo, E., Rasmadi, M., and Tsuruta, H.: Greenhouse gas emissions from tropical peatlands of Kalimantan, Indonesia, Nutrient Cycling in Agroecosystems, 71, 73-80, 2005.

Hall, S. J., and Matson, P. A.: Nitrogen oxide emissions after nitrogen additions in tropical forests, Nature, 400, 152-155, 1999.

Hansen, S.: Daisy, a flexible soil-plant-atmosphere system model, Report. Dept. Agric, 2002.

Heinen, M.: Simplified denitrification models: overview and properties, Geoderma, 133, 444-463, 2006.

Hoeft, I., Steude, K., Wrage, N., and Veldkamp, E.: Response of nitrogen oxide emissions to grazer species and plant species composition in temperate agricultural grassland, Agriculture, ecosystems & environment, 151, 34-43, 2012.

Holland, E., Lee-Taylor, J., Nevison, C., and Sulzman, J.: Global N Cycle: Fluxes and N_2O mixing ratios originating from human activity, Data set. Available on-line: http://www. daac. ornl. gov from Oak Ridge National Laboratory Distributed Active Archive Center, Oak Ridge, Tennessee, USA, doi, 10, 2005.

Holtgrieve, G. W., Jewett, P. K., and Matson, P. A.: Variations in soil N cycling and trace gas emissions in wet tropical forests, Oecologia, 146, 584-594, 2006.

Horváth, L., Führer, E., and Lajtha, K.: Nitric oxide and nitrous oxide emission from Hungarian forest soils; linked with atmospheric N-deposition, Atmospheric Environment, 40, 7786-7795, 2006.

Hu, M., Chen, D., and Dahlgren, R. A.: Modeling nitrous oxide (N_2O) emission from rivers: A global assessment, Global Change Biology, 2016.

Hurtt, G., Chini, L. P., Frolking, S., Betts, R., Feddema, J., Fischer, G., Fisk, J., Hibbard, K., Houghton, R., and Janetos, A.: Harmonization of land-use scenarios for the period 1500–2100: 600 years of global gridded annual land-use transitions, wood harvest, and resulting secondary lands, Climatic Change, 109, 117-161, 2011.

Huttunen, J. T., Alm, J., Liikanen, A., Juutinen, S., Larmola, T., Hammar, T., Silvola, J., and Martikainen, P. J.: Fluxes of methane, carbon dioxide and nitrous oxide in boreal lakes and potential anthropogenic effects on the aquatic greenhouse gas emissions, Chemosphere, 52, 609-621, 2003.

Intergovernmental Panel on Climate Change (IPCC) Revised 1996 IPCC Guidelines for National Greenhouse Gas Inventories vol 1/3 ed J T Houghton, L G Meira Filho, B Lim, K Treanton, I Mamaty, Y Bonduki, D J Griggs and B A Callander (London: IPCC, OECD and IEA), 1997.

Jung, M., Henkel, K., Herold, M., and Churkina, G.: Exploiting synergies of global land cover products for carbon cycle modeling, Remote Sensing of Environment, 101, 534-553, 2006.

Keller, M., and Reiners, W. A.: Soil- atmosphere exchange of nitrous oxide, nitric oxide, and methane under secondary succession of pasture to forest in the Atlantic lowlands of Costa Rica, Global Biogeochemical Cycles, 8, 399-409, 1994.

Kitzler, B., Zechmeister-Boltenstern, S., Holtermann, C., Skiba, U., and Butterbach-Bahl, K.: Nitrogen oxides emission from two beech forests subjected to different nitrogen loads, Biogeosciences, 3, 293-310, 2006.

Kroeze, C., Mosier, A., and Bouwman, L.: Closing the global N_2O budget: a retrospective analysis 1500–1994, Global Biogeochemical Cycles, 13, 1-8, 1999.

van Lent, J., Hergoualc'h, K., and Verchot, L.: Reviews and syntheses: Soil N_2O and NO emissions from land use and land use change in the tropics and subtropics: a meta-analysis, Biogeosciences, 12, 2015.

Liu, M., Tian, H., Yang, Q., Yang, J., Song, X., Lohrenz, S. E., and Cai, W. J.: Long- term trends in evapotranspiration and runoff over the drainage basins of the Gulf of Mexico during 1901–2008, Water Resources Research, 49, 1988-2012, 2013.

Lu, C., and Tian, H.: Net greenhouse gas balance in response to nitrogen enrichment: perspectives from a coupled biogeochemical model, Global Change Biology, 19, 571-588, 2013.

Luizão, F., Matson P., Livingston G., Luizao R. and Vitousek P.M.: Nitrous oxide flux following tropical land clearing, Global Biogeochemical Cycle, 3:281-285, 1989.

Machida, T., Nakazawa, T., Fujii, Y., Aoki, S., and Watanabe, O.: Increase in the atmospheric nitrous oxide concentration during the last 250 years, Geophysical Research Letters, 22, 2921-2924, 1995.

Martikainen, P. J., Nykänen, H., Crill, P., and Silvola, J.: Effect of a lowered water table on nitrous oxide fluxes from northern peatlands, Nature, 366, 51-53, 1993.

Mertz, O., Müller, D., Sikor, T., Hett, C., Heinimann, A., Castella, J.-C., Lestrelin, G., Ryan, C. M., Reay, D. S., Schmidt-Vogt, D., Danielsen, F., Theilade, I., Noordwijk, M. v., Verchot, L. V., Burgess, N. D., Berry, N. J., Pham, T. T., Messerli, P., Xu, J., Fensholt, R., Hostert, P., Pflugmacher, D., Bruun, T. B., Neergaard, A. d., Dons, K., Dewi, S., Rutishauser, E., Sun, and Zhanli: The forgotten D: challenges of addressing forest degradation in

complex mosaic landscapes under REDD+, Geografisk Tidsskrift-Danish Journal of Geography, 112, 63-76, 10.1080/00167223.2012.709678, 2012.
Morse, J. L., Durán, J., Beall, F., Enanga, E. M., Creed, I. F., Fernandez, I., and Groffman, P. M.: Soil denitrification fluxes from three northeastern North American forests across a range of nitrogen deposition, Oecologia, 177, 17-27, 2015.
Mosier, A., Morgan, J., King, J., Lecain, D., and Milchunas, D.: Soil-atmosphere exchange of CH_4, CO_2, NO_x, and N_2O in the Colorado shortgrass steppe under elevated CO_2, Plant and Soil, 240, 201-211, 2002.
Myhre, G., Shindell, D., Bréon, F., Collins, W., Fuglestvedt, J., Huang, J., Koch, D., Lamarque, J., Lee, D., and Mendoza, B.: Anthropogenic and natural radiative forcing, Climate Change, 423, 2013.
NOAA2006A: Combined Nitrous Oxide data from the NOAA/ESRL Global Monitoring Division, 2016.
Pan, S., Tian, H., Dangal, S. R., Zhang, C., Yang, J., Tao, B., Ouyang, Z., Wang, X., Lu, C., and Ren, W.: Complex Spatiotemporal Responses of Global Terrestrial Primary Production to Climate Change and Increasing Atmospheric CO_2 in the 21 st Century, PloS one, 9, e112810, 2014.
Pan, S., Tian, H., Dangal, S. R., Yang, Q., Yang, J., Lu, C., Tao, B., Ren, W., and Ouyang, Z.: Responses of global terrestrial evapotranspiration to climate change and increasing atmospheric CO_2 in the 21st century, Earth's Future, 3, 15-35, 2015.
Prather, M. J., and Hsu, J.: Coupling of nitrous oxide and methane by global atmospheric chemistry, Science, 330, 952-954, 2010.
Prather, M. J., Holmes, C. D., and Hsu, J.: Reactive greenhouse gas scenarios: Systematic exploration of uncertainties and the role of atmospheric chemistry, Geophysical Research Letters, 39, 2012.
Prather, M. J., Hsu, J., DeLuca, N. M., Jackman, C. H., Oman, L. D., Douglass, A. R., Fleming, E. L., Strahan, S. E., Steenrod, S. D., and Søvde, O. A.: Measuring and modeling the lifetime of nitrous oxide including its variability, Journal of Geophysical Research: Atmospheres, 120, 5693-5705, 2015.
Rahn, T., and Wahlen, M.: A reassessment of the global isotopic budget of atmospheric nitrous oxide, Global Biogeochemical Cycles, 14, 537-543, 2000.
Ravishankara, A., Daniel, J. S., and Portmann, R. W.: Nitrous oxide (N_2O): the dominant ozone-depleting substance emitted in the 21st century, Science, 326, 123-125, 2009.
Reay, D. S., Davidson, E. A., Smith, K. A., Smith, P., Melillo, J. M., Dentener, F., and Crutzen, P. J.: Global agriculture and nitrous oxide emissions, Nature Climate Change, 2, 410-416, 2012.
Ren, W., Tian, H., Xu, X., Liu, M., Lu, C., Chen, G., Melillo, J., Reilly, J., and Liu, J.: Spatial and temporal patterns of CO_2 and CH_4 fluxes in China's croplands in response to multifactor environmental changes, Tellus B, 63, 222-240, 2011.
Rochette, P., Angers, D. A., Bélanger, G., Chantigny, M. H., Prévost, D., and Lévesque, G.: Emissions of N O from Alfalfa and Soybean Crops in Eastern Canada, Soil Science Society of America Journal, 68, 493-506, 2004.
Sawamoto, T., Nakajima, Y., Kasuya, M., Tsuruta, H., and Yagi, K.: Evaluation of emission factors for indirect N_2O emission due to nitrogen leaching in agro- ecosystems, Geophysical Research Letters, 32, 2005.
Schmidt, I., van Spanning, R. J., and Jetten, M. S.: Denitrification and ammonia oxidation by Nitrosomonas europaea wild-type, and NirK-and NorB-deficient mutants, Microbiology, 150, 4107-4114, 2004.
Scholes, M., Martin, R., Scholes, R., Parsons, D., and Winstead, E.: NO and N_2O emissions from savanna soils following the first simulated rains of the season, Nutrient Cycling in Agroecosystems, 48, 115-122, 1997.
Smith, K. A., and Arah, J.: Losses of nitrogen by denitrification and emissions of nitrogen oxides from soils, Proceedings-Fertiliser Society, 1990.

Spahni, R., Chappellaz, J., Stocker, T. F., Loulergue, L., Hausammann, G., Kawamura, K., Flückiger, J., Schwander, J., Raynaud, D., and Masson-Delmotte, V.: Atmospheric methane and nitrous oxide of the late Pleistocene from Antarctic ice cores, Science, 310, 1317-1321, 2005.

Stehfest, E., and Bouwman, L.: N_2O and NO emission from agricultural fields and soils under natural vegetation: summarizing available measurement data and modeling of global annual emissions, Nutrient Cycling in Agroecosystems, 74, 207-228, 2006.

Syakila, A., and Kroeze, C.: The global nitrous oxide budget revisited, Greenhouse Gas Measurement and Management, 1, 17-26, 2011.

Thompson, R. L., Ishijima, K., Saikawa, E., Corazza, M., Karstens, U., Patra, P. K., Bergamaschi, P., Chevallier, F., Dlugokencky, E., and Prinn, R. G.: TransCom N_2O model inter-comparison–Part 2: Atmospheric inversion estimates of N_2O emissions, Atmospheric chemistry and physics, 14, 6177-6194, 2014.

Tian, H., Xu, X., Liu, M., Ren, W., Zhang, C., Chen, G., and Lu, C.: Spatial and temporal patterns of CH_4 and N_2O fluxes in terrestrial ecosystems of North America during 1979–2008: application of a global biogeochemistry model, Biogeosciences, 7, 2673-2694, 2010.

Tian, H., Xu, X., Lu, C., Liu, M., Ren, W., Chen, G., Melillo, J., and Liu, J.: Net exchanges of CO_2, CH_4, and N_2O between China's terrestrial ecosystems and the atmosphere and their contributions to global climate warming, Journal of Geophysical Research: Biogeosciences, 116, 2011.

Tian, H., Chen, G., Zhang, C., Liu, M., Sun, G., Chappelka, A., Ren, W., Xu, X., Lu, C., and Pan, S.: Century-scale responses of ecosystem carbon storage and flux to multiple environmental changes in the southern United States, Ecosystems, 15, 674-694, 2012.

Tian, H., Chen, G., Lu, C., Xu, X., Ren, W., Zhang, B., Banger, K., Tao, B., Pan, S., and Liu, M.: Global methane and nitrous oxide emissions from terrestrial ecosystems due to multiple environmental changes, Ecosystem Health and Sustainability, 1, 1-20, 2015.

Tian, H., Lu, C., Ciais, P., Michalak, A. M., Canadell, J. G., Saikawa, E., Huntzinger, D. N., Gurney, K. R., Sitch, S., and Zhang, B., J. Yang, P. Bousquet, L. Bruhwiler, G. Chen, E. Dlugokencky, P. Friedlingstein, J. Melillo, S. Pan, B. Poulter, R. Prinn, M. Saunois, C.R. Schwalm, S.C. Wofsy: The terrestrial biosphere as a net source of greenhouse gases to the atmosphere, Nature, 531, 225-228, 2016.

Vitousek, P. M., Menge, D. N., Reed, S. C., and Cleveland, C. C.: Biological nitrogen fixation: rates, patterns and ecological controls in terrestrial ecosystems, Philosophical Transactions of the Royal Society of London B: Biological Sciences, 368, 20130119, 2013.

Volk, C., Elkins, J., Fahey, D., Dutton, G., Gilligan, J., Loewenstein, M., Podolske, J., Chan, K., and Gunson, M.: Evaluation of source gas lifetimes from stratospheric observations, Journal of Geophysical Research: Atmospheres, 102, 25543-25564, 1997.

Wei, Y., Liu, S., Huntzinger, D. N., Michalak, A., Viovy, N., Post, W., Schwalm, C. R., Schaefer, K., Jacobson, A., and Lu, C.: The North American Carbon Program Multi-scale Synthesis and Terrestrial Model Intercomparison Project–Part 2: Environmental driver data, Geoscientific Model Development, 7, 2875-2893, 2014.

Sun, X. Y., and Xu, H. C.: Emission flux of nitrous oxide from forest soils in Beijing, Scientia Silvae Sinicae, 37, 57-63, 2001.

Werner, C., Butterbach- Bahl, K., Haas, E., Hickler, T., and Kiese, R.: A global inventory of N_2O emissions from tropical rainforest soils using a detailed biogeochemical model, Global Biogeochemical Cycles, 21, 2007.

Wrage, N., Velthof, G., Van Beusichem, M., and Oenema, O.: Role of nitrifier denitrification in the production of nitrous oxide, Soil biology and Biochemistry, 33, 1723-1732, 2001.

Xu, X., H. Tian, M. Liu, W. Ren, G. Chen and C. Lu and C. Zhang. Multiple-factor controls on terrestrial N_2O flux over North America. *Biogeosciences* 9, 1351-1366, 2012.

Yang, Q., Tian, H., Friedrichs, M. A., Hopkinson, C. S., Lu, C., and Najjar, R. G.: Increased nitrogen export from eastern North America to the Atlantic Ocean due to climatic and anthropogenic changes during 1901–2008, Journal of Geophysical Research: Biogeosciences, 120, 1046-1068, 2015.

Zhang, B., Tian, H., Lu, C., Dangal, S. R. S., Yang, J., and Pan, S.: Manure nitrogen production and application in cropland and rangeland during 1860–2014: A 5-minute gridded global data set for Earth system modeling, Earth System Science Data Discussion, in review, 2017.

Zhang, B., Tian, H., Ren, W., Tao, B., Lu, C., Yang, J., Banger, K., and Pan, S.: Methane emissions from global rice fields: Magnitude, spatiotemporal patterns, and environmental controls, Global Biogeochemical Cycles, 2016.

Zhuang, Q., Lu, Y., and Chen, M.: An inventory of global N_2O emissions from the soils of natural terrestrial ecosystems, Atmospheric Environment, 47, 66-75, 2012.

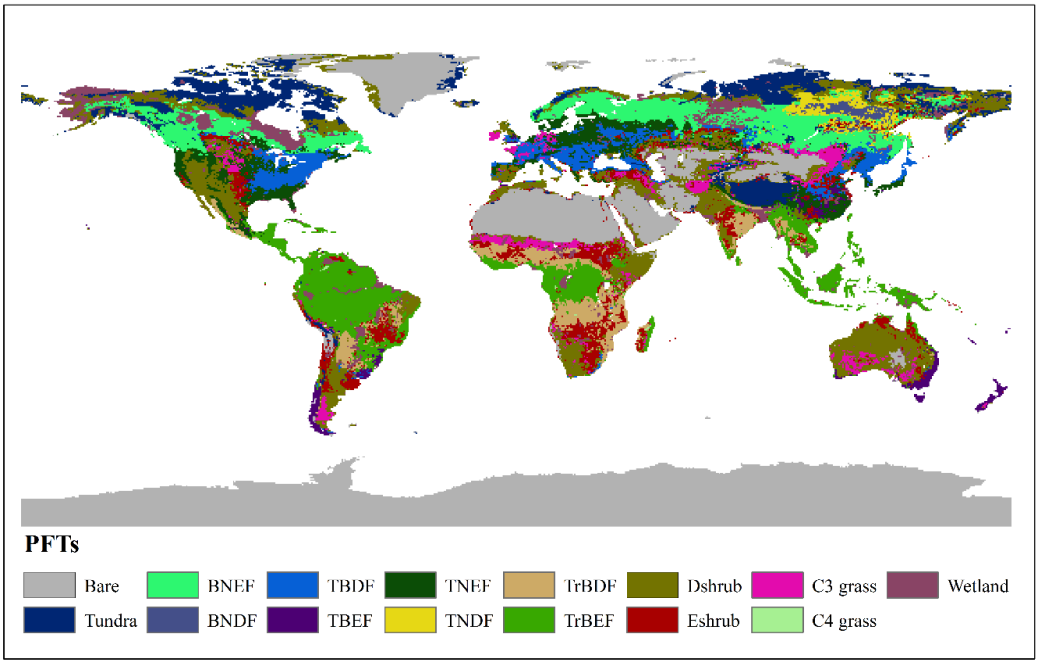

Fig. 1 Global potential natural vegetation map in the pre-industrial era used by DLEM. BNEF: Boreal Needleleaf Evergreen Forest, BNDF: Boreal Needleleaf Deciduous Forest, TBDF: Temperate Broadleaf Deciduous Forest, TBEF: Temperate Broadleaf Evergreen Forest, TNEF: Temperate Needleleaf Evergreen Forest, TNDF: Temperate Needleleaf Deciduous Forest, TrBDF: Tropical Broadleaf Deciduous Forest, TrBEF: Tropical Broadleaf Evergreen Forest, Dshrub: Decidous Shrubland, Eshrub: Evergreen Shrubland.

618

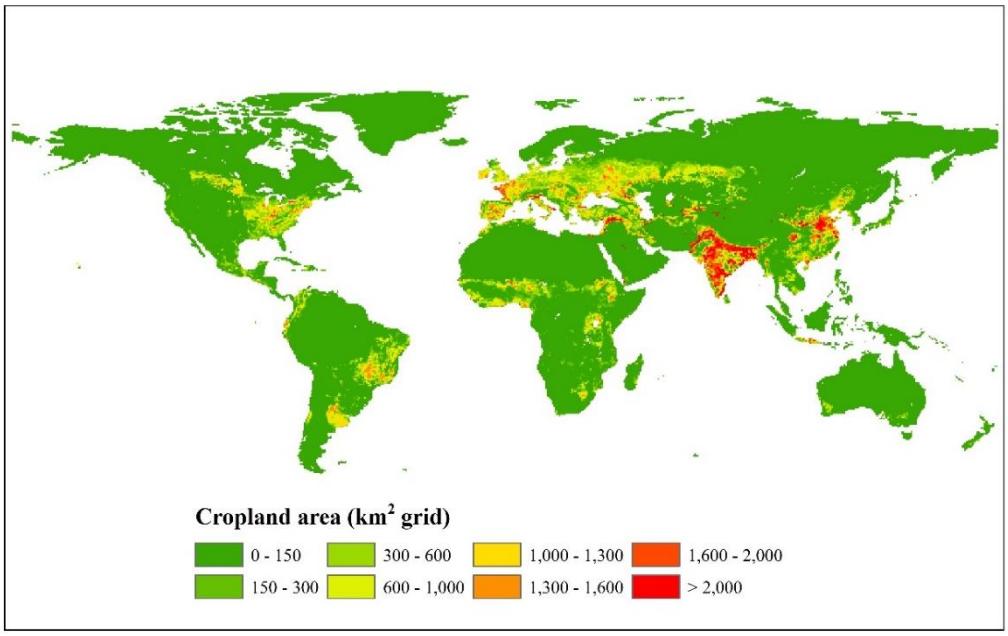

619

620 **Fig. 2** The spatial distribution of cropland area in the year1860.

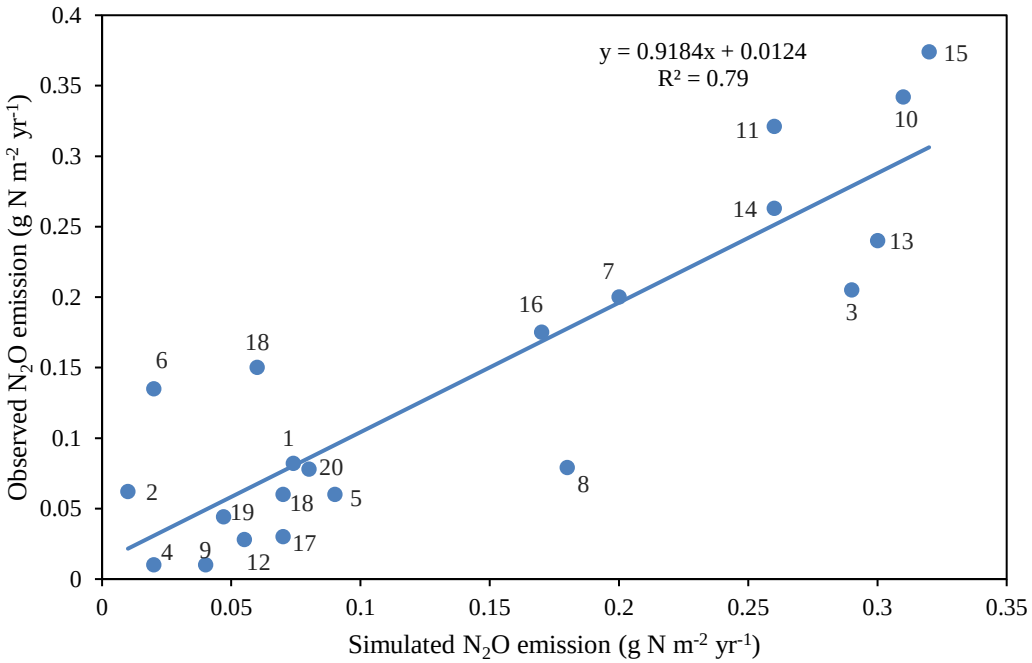

Fig. 3 The comparison of the DLEM-simulated N_2O emissions with field observations. All sites were described in the supplementary material (Table S1).

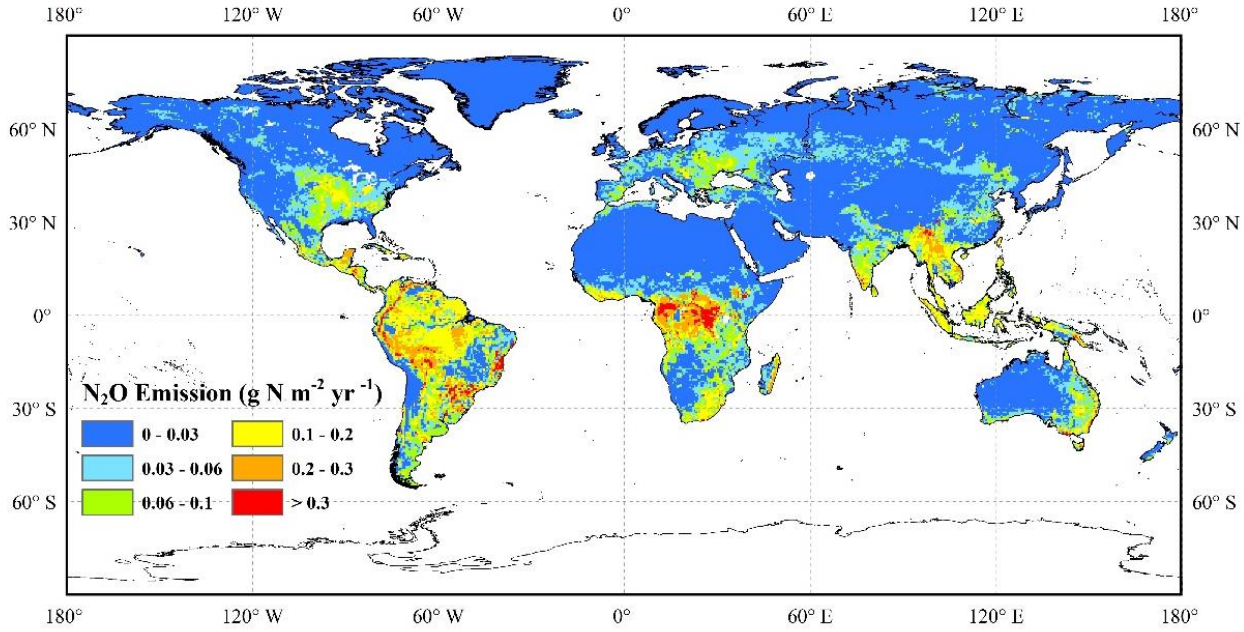

Fig. 4 The spatial distribution of N_2O emission in the pre-industrial era.

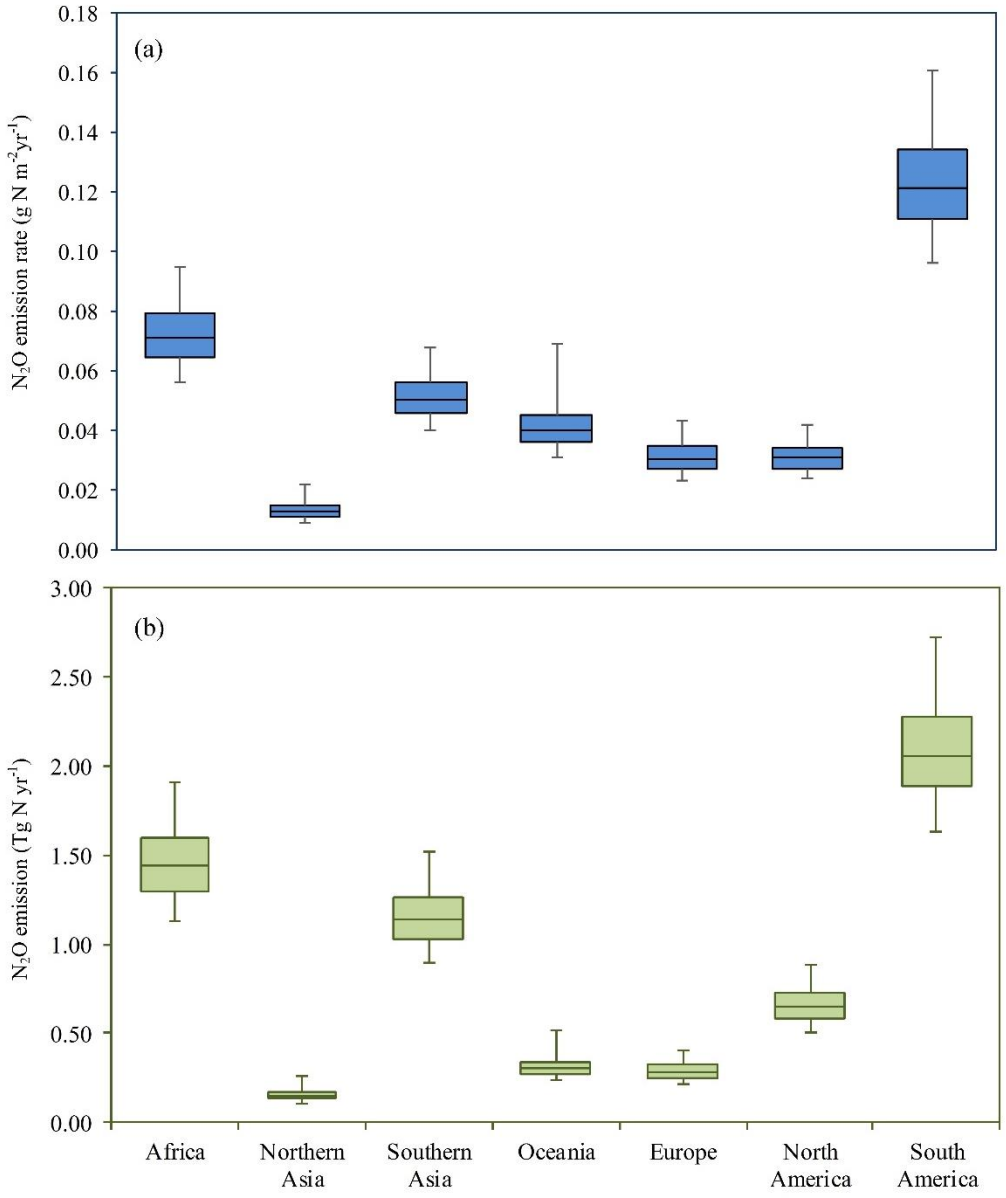

630

631 **Fig. 5** Estimated N_2O emission rates (a) and emissions (b) with uncertainty ranges at continental-level in the year 1860. Solid
632 line within each box refers to the median value of N_2O emission rate or amount.

633

634

635

636

637

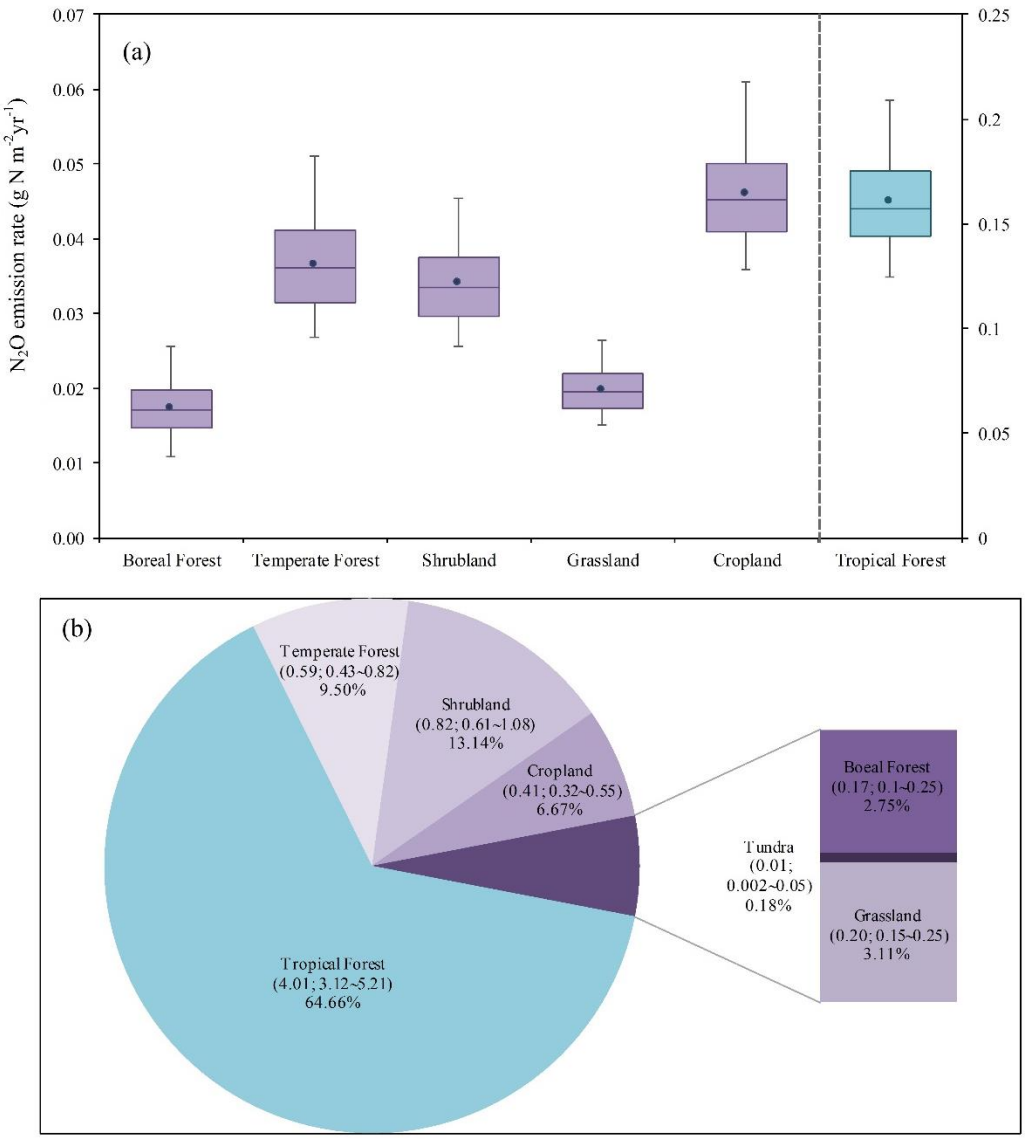

Fig. 6 (a) Estimated N_2O emission rate at biome-level in the year 1860 with the median value (solid line), the mean (solid dot), and the uncertainty range of emission rates from different biomes. The emission rate in the tundra was removed because of the extremely small value (less than 0.003g N $m^{-2}yr^{-1}$); (b) Estimated N_2O emission (Tg N yr^{-1}) with uncertainty ranges and its percentage (%) at biome-level in the year 1860.

Table 1. Pre-industrial N_2O emissions from natural vegetation and croplands in different countries. 1Mha = 10^4 km^2

Country	Vegetation area (Mha)	Natural soils (Gg N yr^{-1})	Cropland (Gg N yr^{-1})	Total (Gg N yr^{-1})
China	756.3	188	62	250
India	306.8	121	64	185
United States	913.9	296	81	377
Pakistan	65.1	5	6	11
Indonesia	174.1	181	2	183
France	52.3	7	9	16
Brazil	835.1	1017	11	1028
Canada	914.6	94	2	96
Germany	36.0	9	4	13
Turkey	74.3	17	11	28
Mexico	191.0	118	3	121
Vietnam	31.7	41	2	43
Spain	48.2	14	6	20
Russian Federation	1575.3	234	19	253
Bangladesh	12.4	2	5	7
Thailand	49.3	56	3	59